# Late Miocene submarine volcanism in ANDRILL AND-1B drill core, Ross Embayment, Antarctica

**Alessio Di Roberto[1], Massimo Pompilio[1], and Thomas I. Wilch[2]**
[1]*Istituto Nazionale di Geofisica e Vulcanologia, sezione di Pisa, Via della Faggiola, 32-56126 Pisa, Italy*
[2]*Department of Geological Sciences, Albion College, 611 E. Porter Street, Albion, Michigan 49224, USA*

## ABSTRACT

**The ANDRILL McMurdo Ice Shelf initiative recovered a 1285-m-long core (AND-1B) composed of cyclic glacimarine sediments with interbedded volcanic deposits. The thickest continuous volcanic sequence by far is ~175 m long and is found at mid-core depths from 584.19 to 759.32 m below seafloor. The sequence was logged, and initial interpretations of lithostratigraphic subdivisions were made on ice during drilling in late 2006. Subsequent observations, based on image, petrographic, and scanning electron microscopy–energy dispersive spectroscopy analyses, provide a more detailed, revised interpretation of a thick submarine to emergent volcanic succession.**

**The sequence is subdivided into two main subsequences on the basis of sediment composition, texture, and alteration style. The ~70-m-thick lower subsequence consists mostly of monothematic stacked volcanic-rich mudstone and sandstone deposits, which are attributed to epiclastic gravity flow turbidite processes. This subsequence is consistent with abundant active volcanism that occurred at a distal site with respect to the drill site. The ~105-m-thick upper subsequence consists mainly of interbedded tuff, lapilli tuff, and volcanic diamictite. A Late Miocene (6.48 Ma) 2.81-m-thick subaqueously emplaced lava flow occurs within the second subsequence. This second subsequence is attributed to recurring cycles of submarine to emergent volcanic activity that occurred proximal to the drill site. This new data set provides (1) the first rock evidence of significant Late Miocene submarine volcanic activity in the Ross Embayment during a period of no to limited glaciation, and (2) a rich stratigraphic record that elucidates submarine volcano-sedimentary processes in an offshore setting.**

## INTRODUCTION

The ANDRILL (Antarctic Geological Drilling Program) AND-1B core provides a well-preserved (>98% core recovery), high-resolution, late Neogene record from the nearshore glacimarine environment in Antarctica (Naish et al., 2007, 2009). The marine core was obtained from beneath the McMurdo Ice Shelf, in the Ross Embayment of Antarctica (Fig. 1). The McMurdo Ice Shelf drill site is located ~10 km east of Hut Point Peninsula, Ross Island (Fig. 1), in the subsidence moat created by the volcanic Ross Island (Naish et al., 2007). The core top is situated 943 m below sea level. The core (Fig. 2) consists of intercalated glacigenic, biogenic, and volcanic deposits, which have been interpreted in terms of changing environmental conditions since ca. 12 Ma (McKay et al., 2009; Naish et al., 2009). Volcanic rocks form a significant component of the core: more than 65,000 of the >2 mm clasts (70% of total clast count) are volcanic (Pompilio et al., 2007), and abundant volcanic layers occur throughout the core with thicknesses ranging from millimeters to 175 m. This study focuses on the 175-m-long volcanic interval from 584.19 to 759.32 mbsf (meters below seafloor), which was classified in the initial report core log record as lithostratigraphic unit 5 (LSU 5) by Krissek et al. (2007).

The AND-1B core stratigraphic sequence was initially subdivided into eight lithostratigraphic units (LSU 1– LSU 8) composed of several depositional sediment facies. Among the eight, LSU 5 (Fig. 2) is distinctive on the basis of its high volcanic content, lack of diatomite, and varied range of siliciclastic sediments (Krissek et al., 2007). LSU 5 includes different depositional facies, the products of which can be attributed to both reworked and primary volcanic depositional processes. Preliminary paleomagnetic studies of the AND-1B core carried out on ice (Wilson et al., 2007b) revealed that LSU 5 covers a time span of at least several hundreds of thousands of years, as at least five inversions of the magnetic polarity occur in this interval. A 2.81-m-thick intermediate lava flow at 646.5–649.2 mbsf was dated to 6.48 ± 0.13 Ma and provides the only isotopic age of the interval (Wilson et al., 2007c). Initial interpretations of the core were based solely on core logging done during drilling. Here we provide a more detailed and refined interpretation of LSU 5, based on reanalysis of the original nongenetic core log descriptions and the actual core, as well as new analysis of accurate high-resolution digital core images and petrographic thin sections. We describe and discuss primary subaqueous volcanic deposits as well as volcanic-rich epiclastic debris in LSU 5 and examine facies relations within a vertical sequence. Interpretations of eruptive and depositional processes for both pyroclastic and epiclastic debris define the evolution of this thick volcaniclastic sequence. The 175-m-thick interval records intense subaqueous volcanic activity during a period of limited to no glaciation.

## EREBUS VOLCANIC PROVINCE

The AND-1B drill site is located in the Erebus Volcanic Province (Fig. 1), which comprises alkaline Neogene volcanic centers on the west flank of the intracontinental West Antarctic rift system in the McMurdo Sound region (Kyle, 1990). Ross Island, a large volcanic complex just north of the drill site, is dominated by the active 3794 m Mount Erebus, surrounded radially by the Mount Terror, Mount Bird, and Hut Point Peninsula eruptive centers (Fig. 1). Mount Erebus is composed mostly of basanite and its fractionated product phonolite (Kyle, 1977, 1981; Kyle et al., 1992); the oldest Erebus outcrops are low-elevation 1.3 Ma Cape Barne rock (Esser et al., 2004). Mount Bird and Mount Terror are basanitic shield volcanoes that erupted 4.6–3.8 Ma and 1.7–1.3 Ma, respectively (Wright and Kyle, 1990a, 1990b;

*Geosphere*; October 2010; v. 6; no. 5; p. 524–536; doi: 10.1130/GES00537.1; 6 figures; 1 table; 4 supplemental figures.

Kyle and Muncy, 1989). Hut Point Peninsula, located just 10 km west of the drill site, is the most proximal subaerial volcanic outcrop to the drill site. Surface mapping and drill core records from the 1970s at Hut Point Peninsula reveal a Pleistocene (since 1.3 Ma) record of evolving alkaline volcanism, dominated by basanitic-hawaiitic cinder cones and a phonolite dome at the surface (Kyle, 1981).

Major volcanic centers are also located south of the AND-1B drill site. White Island, the magmatism of which dates to 7.7 Ma, is a basanite to tephriphonolite shield volcano and is the next most proximal volcano, located 15 km south-southeast of the drill site (Cooper et al., 2007). Farther south (40–60 km from the drill site), Black Island, Minna Bluff, Mount Morning, and Mount Discovery are all major volcanic centers. The earliest known volcanic outcrops date to 18.7 Ma and include extensive evolved alkaline explosive vent complexes on the northwestern and northeastern slopes of Mount Morning (Martin et al., 2009) and farther south, at Mason Spur and Helms Bluff (Armstrong, 1978; Kyle and Muncy, 1989; Kyle, 1990). A thick pumice lapilli tuff, dated to 22 Ma, was also found in the Cape Roberts Project CRP-2 drill hole (Armienti, et al., 2001; McIntosh, 2001). Late Miocene volcanism with ages similar to the ca. 6.5 Ma lava flow in LSU 5 is known to have occurred at both White Island and Minna Bluff. Minna Bluff, south of the drill site, formed between 12 and 6 Ma and has since acted as an important barrier to the flow of the Ross Ice Shelf into McMurdo Sound (Wilch et al., 2008; Talarico and Sandroni, 2009). Glacial reconstructions show that flowlines of a grounded ice sheet in the Ross Embayment directed to the drill site would sweep around Minna Bluff (12–6 Ma) and past White Island (7.7–0.2 Ma) (Naish et al., 2009). Two major glacial unconformities dated as 9.6 and ca. 10.4 Ma on Minna Bluff are attributed to erosion by an early Ross Ice Sheet (Fargo et al., 2008). Talarico and Sandroni (2009) suggested that clasts from both Minna Bluff and White Island are important components of glacial deposits in the AND-1B core.

Recent aeromagnetic studies have also suggested the possible existence of submarine volcanoes beneath the McMurdo Ice Shelf, as well

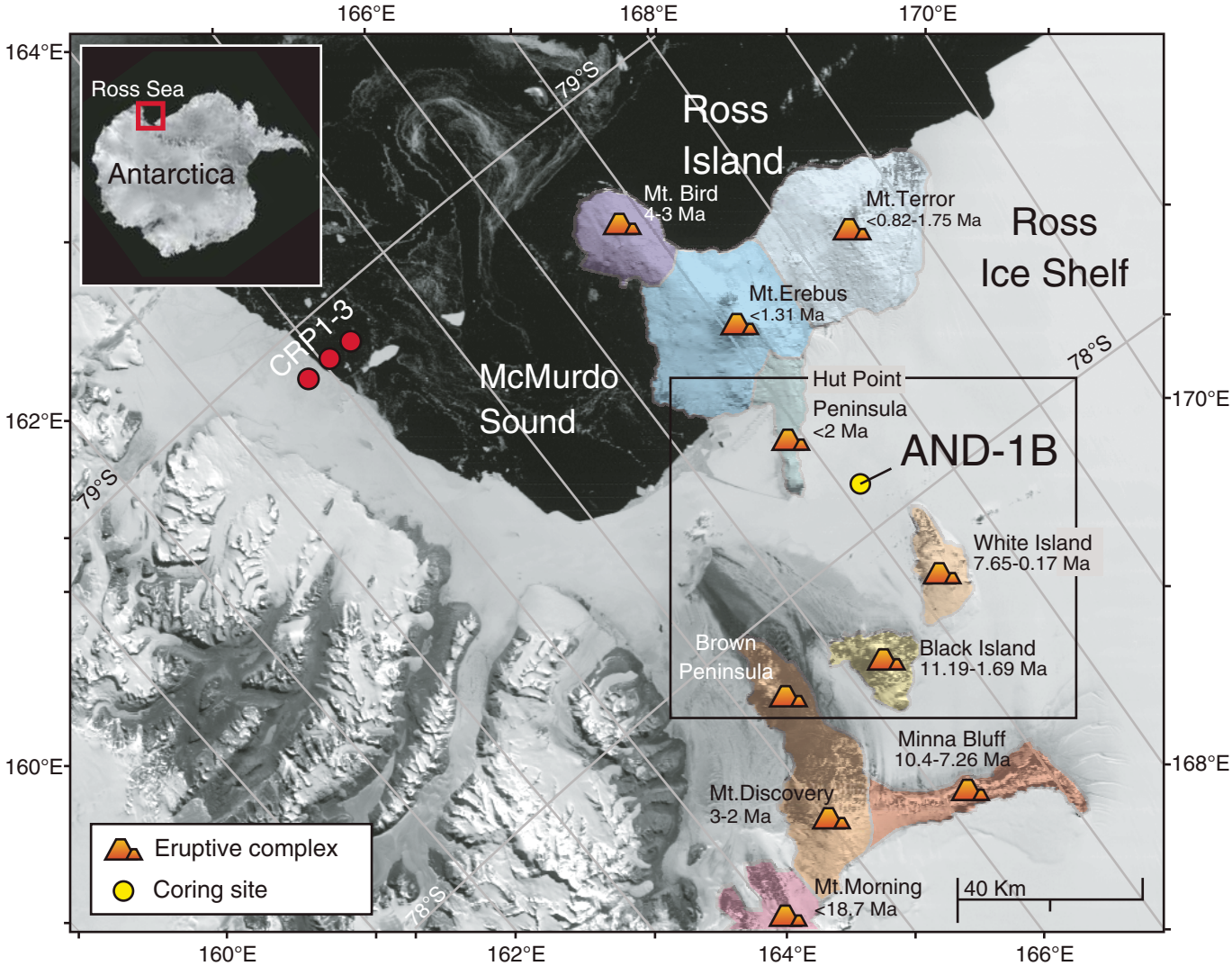


**Figure 1. Location of the core site and main geographical features of the Erebus Volcanic Province. Map also shows volcanic centers (encircled with different colors) belonging to the Erebus Volcanic Province with relative time span of activity. Satellite image from SSEC/UW-Madison AWS Network (Space Science and Engineering Center, University of Wisconsin Automatic Weather Station, http://amrc.ssec.wisc.edu/). CRP1–3—Location of Cape Roberts Project 1–3 drill holes. The box indicates the area described in Figure 5.**

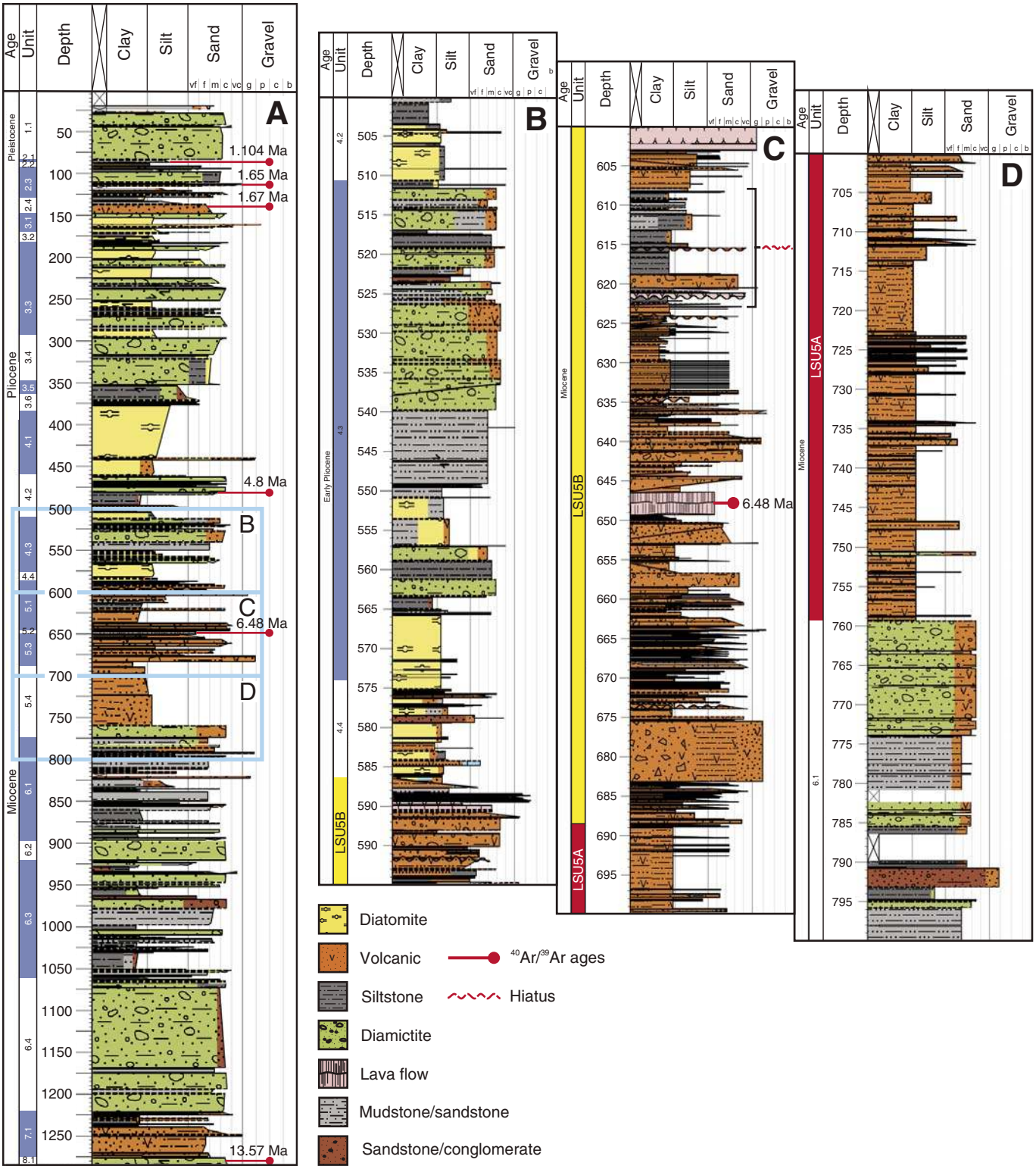


**Figure 2. Stratigraphic summary of the AND-1B core from 500 to 800 m below seafloor (mbsf). Lithologies are plotted against depth.**

TABLE 1. LITHOFACIES DESCRIPTION AND INTERPRETATION OF DEPOSITIONAL PROCESS

| Facies | Bed description | Components | Volcanic/Glacial process |
|---|---|---|---|
| 2 to 6 Volcanic-rich mudstone to sandstone | Cm- to mm-thick beds of siltstone, clayey siltstone, and fine- to medium-grained sandstone, interlaminated and interbedded at millimeter to centimeter scales (supplemental material 1) | Reworked glass shards, pumice and scoria, lava fragments, and magmatic crystals; granitoids, metasediments and mudstone intraclasts | Turbidity currents from a far located grounding |
| 11a - Lapilli Tuff and Tuff | Cm- to dm-thick, massive to crudely stratified, coarse lapilli tuff to fine tuff, normally graded to well-bedded (supplemental material 2) | Pristine pumice, scoria and glass shards; few igneous crystals, and dense, angular lava fragments | High- to low-concentrated, eruption-fed, aqueous density current |
| 11b - Lava Flow | Fine-grained tephrite (supplemental material 3) | N.A. | Submarine lava flow |
| 11c - Volcanic Diamictite | Cm- to m-thick, coarse sand to breccia, massive to very poorly to faintly bedded (supplemental material 4) | Dense, angular lavas, scoria and oxidized altered volcanics | High-density mass flows (debris flows) |

*Note*: N.A.—not available.

as submarine lava flow extensions of exposed volcanic islands including White Island (Wilson et al., 2007a). These inferred submarine volcanoes have not been sampled or dated.

## TECHNIQUES

The AND-1B core was logged first on ice during drilling in late 2006 (Krissek et al., 2007; Pompilio et al., 2007). Core description was conducted by the ANDRILL McMurdo Ice Shelf sedimentology-stratigraphy team, following procedures and operations outlined in the Scientific Logistics Implementation Plan for the ANDRILL McMurdo Ice Shelf Project (SLIP; Naish et al., 2006). Preliminary stratigraphic and petrologic data on volcanic rocks in the AND-1B core were reported in Krissek et al. (2007) and in Pompilio et al. (2007), and provide the starting point for the analysis and interpretations in this study.

Additional macroscopic and stratigraphic descriptions of LSU 5 have been further implemented by analysis of high-resolution digital images (150 dpi) of split drill core visualized in a desktop workstation using Corelyzer software (Rao et al., 2006). These images were studied in order to infer mechanisms of eruption, transport, and deposition. Macroscopic observations of digital images and core were integrated with detailed sample characterization performed on more than 50 thin sections distributed within LSU 5; additional sampling was undertaken where particular structures are evident or in correspondence to specific sedimentary units. Selected sample microtextures and macrotextures were further analyzed using scanning electron microscopy–energy dispersive spectroscopy Philips XL30 scanning electron microscope (accelerating voltage 20 kV, beam current 1 nA, working distance 10 mm), equipped with energy dispersive X-ray analysis (DX 4; Earth Science Department of Pisa University) and backscattered electron images collected with a JEOL JXA 8200 Superprobe (Istituto Nazionale di Geofisica e Vulcanologia, Rome).

## FACIES

Krissek et al. (2007) grouped primary and near-primary volcanic rocks and sediments in a single facies (designated #11 in core logs), which includes lapilli tuff, volcanic diamictite, and a tephritic lava flow. Some of these deposits were interpreted as slightly reworked by sediment gravity flow processes but less reworked than volcanic-rich equivalents of other facies. Volcaniclastic rocks were also included in primarily nonvolcanic siliciclastic facies, including facies #2 (mudstone), #3 (interstratified mudstone and sandstone), #4 (mudstone with interdispersed common clasts), #5 (rhythmically interlaminated mudstone with siltstone or sandstone) and #6 (sandstone) (Krissek et al., 2007). Here we redefine and redescribe these facies in the context of the LSU 5 volcanic interval. On the basis of detailed stratigraphic, textural, and component analyses we subdivided facies 11 into 3 subfacies (11a–11c), keeping the same number for coherence (Table 1; supplemental figures); this further subdivision was considered necessary to detail the complex architecture of LSU 5.

### Facies 2–6: Volcanic-Rich Mudstone to Sandstone

We group the five facies (facies 2–6) identified by Krissek et al. (2007) as products of reworking of primary volcanic deposits into a single facies association (Fig. 3A; Supplemental Figure 1[1]). In the original facies description, these volcanic units were included as variations of facies that were mostly siliciclastic. The lower part of LSU 5 is dominated by these facies (Fig. 4), including dark gray to black, centimeter- to millimeter-thick beds of siltstone, clayey siltstone, and fine- to medium-grained sandstone, interlaminated and interbedded at millimeter to centimeter scales. Beds commonly exhibit normal grading, although nongraded massive beds also occur. Planar lamination and cross-stratification are common while ripple cross-lamination is mostly limited to coarse siltstone. Incomplete Bouma sequences sometimes occur. Basal contacts with underlying sediments are either sharp or diffuse, whereas in the topmost part convolute bedding and fluid escape structures are common.

Sandstone is less common and is mostly represented by volcanic fine- to medium-grained sandstone, which is normally graded to volcanic siltstone; some nongraded massive beds also occur. Incipient planar laminations, cross-stratification, and climbing ripple laminations are common. Basal contacts of sandstone units are usually sharp and interpreted as erosional. The majority of beds are constituted by a heterolithic mix of volcanic-derived clasts (i.e., glass shards, variously vesicular pumices and scoria, dense lava fragments, and magmatic crystals) with variable and sometimes significant amounts of mainly basement-derived clasts (granitoids, metasediments) and mudstone intraclasts. Both volcanic-derived and crystalline rock fragments are subangular to well rounded and show traces of intense reworking by granule abrasion and comminution. Sandstone and siltstone are usually matrix supported; the matrix is composed of silt-sized (tens of microns) volcanic fragments

[1]Supplemental Figure 1. PDF file image of the uppermost half of the core is composed of heterolithic, volcanic-rich, clast-rich muddy diamictite. Beds are composed of granule- to pebble-sized (up to few cm in diameter) clasts of granitoids, metasediments, volcanics, and mudstone intraclasts immersed in a heterolithic, volcanic-rich, sand-sized matrix. This part of the core is well stratified horizontally with stratifications defined by color variation, horizontal alignment of clast long axes, and variations in grain size. The lowermost half of the interval is composed of stacked layers of very dark greenish to black volcanic coarse sandstone with dispersed granules, volcanic fine- to medium-grained sandstone, volcanic fine sandstone, volcanic claystone, volcanic siltstone, weakly stratified silty claystone/clayey siltstone, and volcanic mudstone. If you are viewing the PDF of this paper or reading it offline, please visit http://dx.doi.org/10.1130/GES00537.S1 or the full-text article on www.gsapubs.org to view Supplemental Figure 1.

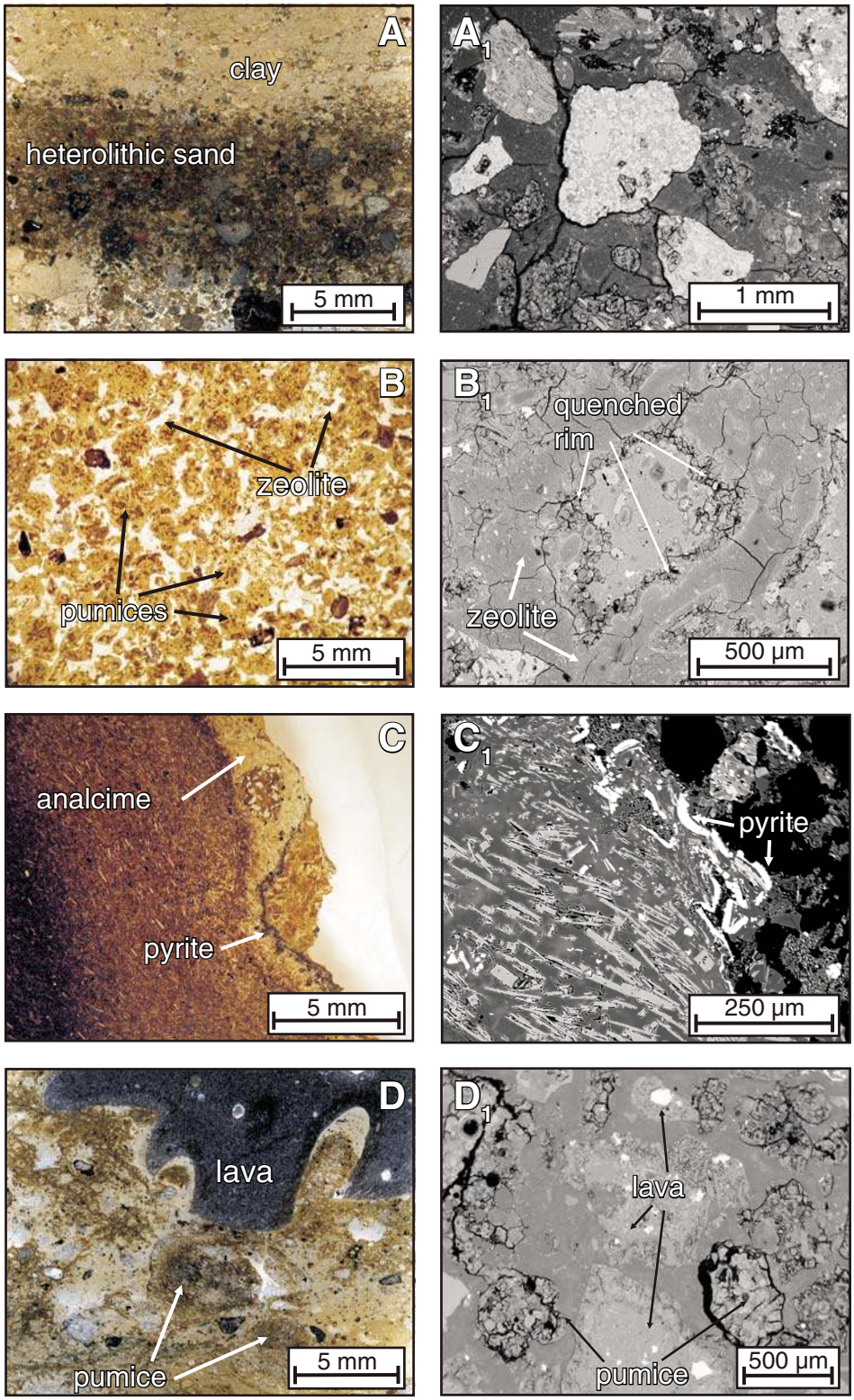


**Figure 3. Thin section optical (left column) and scanning electron microscope backscattered images (right column) of selected representative samples of relevant facies in LSU 5: A and A1—heterolithic epiclastic sandstones (facies 2–6); B and B1—volcanic tuff (facies 11a); C and C1—lava flow (facies 11b); D and D1—volcanic diamictites (facies 11c).**

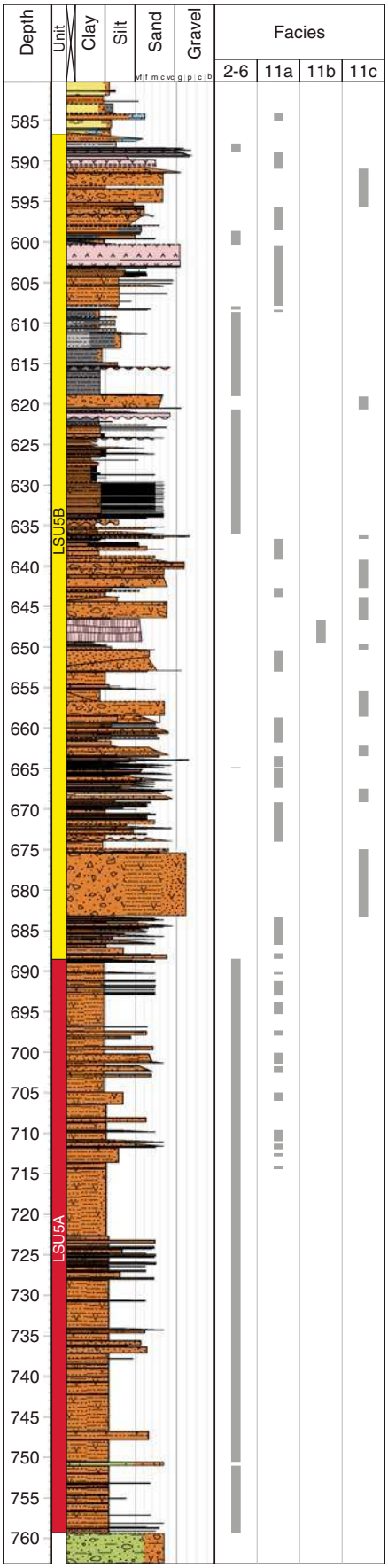


**Figure 4. Composite stratigraphic log of LSU 5A and LSU 5B, showing facies distribution with depth (in mbsf). Lithologies are the same as Figure 2.**

and minerals, clay aggregates, and crystalline to microcrystalline zeolites.

### Facies 11a: Lapilli Tuff and Tuff

Lapilli tuff and tuff (Fig. 3B; Supplemental Figure 2[2]) are one of the most widespread deposits within LSU 5 (Fig. 4). The units are composed of centimeter- to decimeter-thick, massive to crudely stratified, coarse lapilli tuff to fine lapilli tuff (sizes after White and Houghton, 2006) normally graded to or overlain by well-bedded, extremely fine to fine tuff with diffuse parallel to low-angle cross-laminations. The coarser lapilli tuff beds are moderately to poorly sorted and are composed of juvenile greenish-yellowish clasts set in a dark green matrix; they are matrix to clast supported and sorting and/or bedding may be obscured by alteration, although normal grading is obvious in some units. The finer tuff beds are moderately to well sorted, commonly clast supported and open-framework textured, and rarely graded. Juvenile fragments of both lapilli tuff and fine tuff beds are composed of texturally homogeneous pumice, scoria and glass shards mixed with reduced amounts of igneous crystals, and dense, angular lava fragments. Abundant reddish oxidized fragments occur especially in the uppermost part of the sequence. Juvenile fragments are mostly aphyric, with few crystals of plagioclase, pyroxene, amphibole, and altered olivine in a glassy matrix. Some juvenile fragments are tachylitic with abundant microlaths of plagioclase frequently altered and replaced by clay minerals and chlorite.

Within lapilli tuff, volcanic fragments are variably vesicular, likely representing a continuum between end members represented by clasts with low vesicularity made up of few relatively large vesicles (hundreds of microns in diameter) to honeycomb-textured clasts with fine vesicles (few tens of microns in diameter). Vesicles are frequently convoluted and deformed with some clasts showing a probable vesiculation after fragmentation. In these clasts, early syneruptive vesiculation is preserved in vesicles aligned below quenched and fractured clast rims, while post-fragmentation processes give rise to undeformed, mostly spherical vesicles developed in the inner part of the clast. A large portion of fragments exhibit marginal quenching and widespread fracturing. The nature of the vesicularity and quenching, in addition to the presence of fluidal deformation of the thin glass tips, suggests possible heat retention during deposition.

Stratigraphic relationships between mainly massive lapilli tuff and laminated fine tuff intervals are variable. Three main cases occur: (1) deposits with similar proportion of lapilli tuff and tuff (the most common); (2) much reduced portions of lapilli tuff overlain by extensively developed fine tuff; and (3) multiple stacked sequences of lapilli tuff overlain by, and separated by erosion surfaces from, very limited occurrences of fine tuff. Laminated fine-grained tuff is frequently overlain by yellow-gray volcanic siltstone or claystone, which is moderately to intensely bioturbated with frequent convolution, fluid escape structures, and load structures. Coarse tuff is usually cemented by a micritic to crystalline matrix made up by clay and zeolites (mainly analcime and phillipsite). Fine-grained tuff is always cemented by highly crystalline zeolite (phillipsite and analcime).

A few layers of parallel to low-angle laminated, extremely fine, well-sorted tuff also occur just above the top of LSU 5 at 584.19–584.84 mbsf. Although Krissek et al. (2007) ascribed these layers to LSU 4.4, these tuffs can be considered genetically linked to similar deposits of LSU 5. These tuff beds are centimeter to decimeter thick and clast supported, and are composed of y-shaped to blocky, poorly vesicular and aphyric glass shards. Calcite to zeolite crystalline cement constitutes the matrix. Many shards exhibit concentric rims of devitrified glass a few tens of microns thick and in some cases tiny perlitic fractures.

### Facies 11b: Lava Flow

A 2.81-m-thick lava flow occurs within the LSU 5 sequence from 646.49 to 649.30 mbsf (Figs. 3C and 4; Supplemental Figure 3[3]). The lava flow is a fine-grained tephrite, with few large (>1 mm) feldspar phenocrysts set in a pilotaxitic groundmass. The upper lava flow contact exhibits a 1–2-cm-thick alteration rim, composed of a series of concentric rinds of

[2]Supplemental Figure 2. PDF file image of pumiceous lapilli tuff to tuff. Deposits are moderately well sorted and are composed of clasts ranging from coarse ash to lapilli (~1 cm). Lapilli tuff are clast-supported. Although sorting and bedding are partially obscured by alteration, faint normal grading occurs. Few coarse sand-sized grains of red scoria occur in the interval. Clasts are often cemented by calcite. Patches and lenses of pyrite occur. If you are viewing the PDF of this paper or reading it offline, please visit http://dx.doi.org/10.1130/GES00537.S2 or the full-text article on www.gsapubs.org to view Supplemental Figure 2.

calcite and zeolite. Similarly, the basal 2 cm of the flow in contact with underlying sediments are also altered to calcite, zeolite (Krissek et al., 2007), and pyrite. Soft-sediment deformation occurs at the contact between the lava flow and underlying muddy sediments. Abundant millimeter-wide fractures and sparse vesicles are evident within the lava and are now occupied by secondary calcite and silica veins and amygdales. Fractures near the top and base of the lava are generally parallel to the bounding surfaces; fractures in the core of the lava are inclined to anastamosing (Krissek et al., 2007). There is no clear evidence of pillow-like structures in this lava. The occurrence of glassy rinds, flow and shear textures, and the presence of a subaqueous gravity flow just above the lava flow indicate a submarine setting (Pompilio et al., 2007).

### Facies 11c: Volcanic Diamictite

Diamictite (Fig. 3D; Supplemental Figure 4[4]), in which volcanic detritus is dominant, is an important component of the LSU 5 volcanic sequence and represents a variation of the heterolithic facies 9 (stratified diamictite) and 10 (massive diamictite) described by Krissek et al. (2007). Most of the volcanic diamictite is massive, very poorly sorted, and very poorly to faintly bedded, although normal grading appears in some examples. The volcanic diamictites are composed of coarse sand- to pebble-sized clasts of dense, angular lavas with textures analogous to the lava flow, scoria, and oxidized altered volcanics enclosed in a clay- to sand-sized matrix. Some lava clasts have a jig-saw texture, suggesting short transport after breakage; accidental very rounded, yellow claystone intraclasts also occur.

The volcanic diamictite matrix is dark green and dominantly composed of clay- and zeolite-altered volcanic ash. Volcanic diamictite beds are usually <2 m thick (Krissek et al., 2007), but sequences of stacked diamictite beds as thick as 10 m also occur.

## STRATIGRAPHY OF AND-1B: LSU 5

We report here observational data collected off ice, including results from the examination of high-resolution images of the core and analysis of thin sections by optical and scanning electron microscope. This information integrates and expands upon previous on-ice core descriptions summarized in Krissek et al. (2007). The LSU 5 was originally subdivided on ice by the AND-1B sedimentology team into 4 subunits, LSU 5.1–5.4, that were differentiated on the basis of lithostratigraphic characteristics. Here we simplify the model and, on the basis of volcanic and sedimentologic facies analysis (Fig. 4), subdivide the entire LSU 5 into two sequences, LSU 5A and LSU 5B.

### Sequence LSU 5A (688.92–759.32 mbsf: LSU 5.4)

Sequence LSU 5A includes the whole of LSU 5.4 of Krissek et al. (2007) and extends from 688.92 to 759.32 mbsf. It comprises an almost monothematic sequence of siltstone, clayey siltstone, and sandstone belonging to facies 2–6 of Krissek et al. (2007). Beds are volcanic rich throughout LSU 5A, with variable quantities of nonvolcanic, mainly crystalline rock fragments. Crystalline rock fragments are more abundant in some layers in the lowermost meters of the subsequence (e.g., in the volcanic-rich, clast-rich muddy diamictite located at 750.54–751.01 mbsf). Siltstone, clayey siltstone, and sandstone are periodically interrupted by yellowish, millimeter- to centimeter-thick laminae enriched in biogenic silica sediments. Bioturbation is variable and sometimes masked by sediment cementation.

In the uppermost part of LSU 5A (688.92–714.80 mbsf), centimeter- to decimeter-thick beds of lapilli tuff and tuff (facies 11b) are interfingered with laminated sandstone and siltstone. The progressive increase in the number and thickness of tuff beds toward the top of sequence LSU 5A marks the transition into sequence LSU 5B. The passage from sequence LSU 5A to sequence LSU 5B is not marked by a sharp unconformity, hiatus, or erosive surface, and was put at 688.92 mbsf since above this depth tuff beds became predominant.

### Sequence LSU 5B (584.19–688.92 mbsf: LSU 5.3–5.1)

Sequence LSU 5B comprises three of the lithostratigraphic subunits (LSU 5.1–5.3) traced by Krissek et al. (2007), as well as the lowest 2 m of LSU 4.4. The sequence extends from 688.92 to 584.19 mbsf and is largely composed of stacked tuff and lapilli tuff beds (facies 11a) and volcanic diamictite (facies 11c). Intervals of interleaved volcanic-rich sandy claystone and dark sandstone as thick as several meters (facies 3, 4, 5; e.g., between 608.22 and 618.58 mbsf) also occur. Deposits consist of dark olive to gray sandy claystone beds, to 1 m thick, interfingered with millimeter- to centimeter-thick sandstone, laminated to massive and frequently bioturbated, though the dark color may obscure the degree of bioturbation present.

The sequence also includes the 2.81-m-thick lava flow (facies 11b) found from 646.49 to 649.30 mbsf. The lava flow is associated with incipiently bedded, very poorly sorted, and crudely normally graded volcanic diamictites (facies 11c). Volcanic diamictites, to ~8 m thick, are widespread in the sequence even when not associated with a lava flow (e.g., 674.83–683.13, 655.45–658.41, and 618.93–620.50 mbsf).

Several stacked extremely fine tuff layers occur very close to the topmost part of the sequence (584.19–584.84 mbsf) (facies 11b); they are almost completely composed of well-sorted, y-shaped to blocky glass shards with traces of glass hydration, slight glass rim leaching, and pervasive cracks. The deposit is clast supported and cemented with crystalline calcite.

## FACIES INTERPRETATIONS

### Rationale

Submarine, nonwelded pyroclastic debris deposits that are directly related to volcanic explosions are very difficult to discriminate from cold, remobilized, volcanogenic mass flow deposits because of the lack of unequivocal distinctive criteria. The distinction is more difficult where deposits are altered, metamorphosed, and/or deformed as in ancient sequences or where sediment exposure is laterally limited and depositional structures are poorly traceable. Notwithstanding, a number of recent works have demonstrated that discrimination of submarine primary pyroclastic deposits from those subjected to reworking and redeposition (epiclastic) is possible where detailed facies analysis is performed (White, 1996; Skilling, 1994;

[3]Supplemental Figure 3. PDF file image of lava flow. The lava is a fine-grained tephrite, with few large (>1 mm) feldspar phenocrysts set in a pilotaxitic groundmass. The fracture pattern is variable from the top of the interval toward the base. Pyrite coating and secondary minerals are abundant in fractures and vesicles and at the sediment contact. If you are viewing the PDF of this paper or reading it offline, please visit http://dx.doi.org/10.1130/GES00537.S3 or the full-text article on www.gsapubs.org to view Supplemental Figure 3.

[4]Supplemental Figure 4. PDF file image of volcanic diamictite predominantly composed of granule- to small pebble-sized (up to 4 cm in diameter) clasts of pumice, scoria, and lava immersed in sand-sized matrix. The volcanic clasts are subangular to angular; red vesicular scoria are abundant. Beds are faintly stratified horizontally by changes in clast content and dominant clast types at decimetric scale. The matrix of this breccia is mainly composed of pumice sand that typically forms >50% of the matrix but locally exceeds 90%. The matrix also includes zeolites and calcite. If you are viewing the PDF of this paper or reading it offline, please visit http://dx.doi.org/10.1130/GES00537.S4 or the full-text article on www.gsapubs.org to view Supplemental Figure 4.

Smellie and Hole, 1997; Mueller et al., 2000). Moreover the nature, texture, and morphological properties of clasts can be used to help in discriminating the sediment origin.

Basaltic eruptions at shallow to moderate depths, such as those observed at Surtsey Volcano, Iceland (Kokelaar, 1983), Falcon Island, Tonga (Hoffmeister et al., 1929), Capelinhos, Faial Island, Azores (Machado et al., 1962; Cole et al., 1996, 2001; Solgevik et al., 2007; Zanon et al., 2008), Kick'em-Jenny (Lesser Antilles), and the recent eruption off the coast of Nuku'alofa, Tonga (Associated Press, 2009), produce great amounts of fragmental volcanic products. Volcanic rock and detritus can be transferred to the basins either by eruptive or syneruptive processes like subaqueous pyroclastic flows and eruption-fed aqueous density currents. Alternatively, volcanic material temporarily stored on the cone flanks can be redistributed into adjacent basins via gravity flows.

Primary basaltic volcaniclastic deposits produced by recent and ancient mafic underwater eruptions, such as at Greenland (Mueller et al., 2000), are typified by a very homogeneous (monomictic) composition and dominated by a poorly sorted mixture of mafic scoria fragments, glass shards, and crystals. The angular clasts preserve primary fragile structures (e.g., thin glassy rims) and are unabraded. Epiclastic or reworked volcanic-rich deposits, not directly related to a single eruption, may originate from either subaerial pyroclastic sediments or from submarine volcanic flows. Such reworking occurs in particular during periods of quiescence of the eruptive activity. Primary pyroclastic deposits may be eroded and transported by fluvial, marine, and glacial systems. Volcanic fragments occurring in epiclastic deposits usually show traces of intense reworking such as rounding, abrasion, and comminution, and are variably mixed with nonvolcanic material from within the depositional basin, or derived from source rocks outside the basin area, including siliciclastic and crystalline basement rocks and/or bioclastic fragments. Lithological and sedimentological observations indicate that both epiclastic and primary volcaniclastic deposits occur throughout LSU 5 and provide a record of an evolving submarine volcanic complex.

### Sequence LSU 5A: 688.92–759.30 mbsf

A combination of sedimentary structures, including bedding, planar and low-angle cross-stratification, normal grading, partial Bouma sequences, convolute bedding, and rip-up clasts, indicates a turbidity current origin for the majority of sequence LSU 5A. Among turbidites, the dominance of heterolithic siltstone, silty claystone, and sandstone, as well as intense reworking of clasts all point to a prevalent epiclastic origin of sediments. Turbidites may be deposited by turbidity currents resulting from grounding-line fan processes or volcanic and/or tectonic activity. The fine nature of the sediment and the near total absence of dropstones indicate that turbidity currents may develop from a grounding line located far from the drill site and may funnel fine-grained products produced by fluvial and glacial erosion of volcanic and basement rock. Similar deposits may be produced from the mixing of primary submarine volcanic deposits with nonvolcanic detritus; the mixing may occur both prior to or during the transport toward the deeper portion of the sedimentary system, with the nonvolcanic fractions supplied by glacier tongues descending from the Transantarctic Mountain front and by grounding-line processes.

A significant change in depositional environment and processes occurs in the upper part of the LSU 5A sequence. The presence of lapilli tuff and tuff in the upper meters of sequence LSU 5A marks a transition from the predominantly epiclastic sedimentation to a system dominated by materials directly derived from explosive volcanic activity. Though core exposure is limited, the tuff and lapilli tuff deposits are similar to eruption-fed density current deposits in recent or ancient submarine and subglacial explosive volcanic successions in several locations described by several authors (e.g., Fiske, 1963; Mueller and White, 1992; White, 1996; Smellie and Hole, 1997; Fiske et al., 1998; Smellie, 1999; White and Houghton, 1999; White, 2000).

Poorly sorted and massive to crudely stratified lapilli tuff may represent the main body of highly concentrated, eruption-fed, aqueous density currents with high sedimentation rates, whereas the thin-bedded and parallel to low-angle, cross-laminated uppermost part of the tuff may represent deposition by cogenetic low-density flows (White, 2000; Mueller, 2003). These low-density flows may develop in the tail of the eruption-fed aqueous density currents (Kokelaar and Busby, 1992; Martin and White, 2001; Mueller, 2003) or by the collapse of fine sediments injected into the water column by subaqueous pyroclastic jets (the same that generate eruption-fed density currents) (Cashman and Fiske, 1991). The final drape may produce a very fine ash deposit elutriated from the main part of the flow during the transport (Mueller, 2003) and deposited as fallout through the water column.

The interpretation of a primary volcanic density flow origin for these deposits is based on several key features, including the occurrence of very homogeneous components (scoria and dense lava fragments), the almost complete absence of grain abrasion, and the complete preservation of clasts with complex shapes (Doucet et al., 1994; White, 2000). The evidence for heat retention associated with larger clasts during their deposition, i.e., marginal quenching, flattened and convoluted vesicles, and deformation of thin glass tips, supports the hypothesis of a primary deposition of syneruptive hot gravity flows. The presence of sparse tuff in the uppermost part of LSU 5A indicates the initiation of sporadic explosive subaqueous activity close to the drill site. The limited thickness and small grain size of these deposits as well as their intermittent occurrence within the LSU 5A sequence suggest that they resulted from either low-energy eruptive activity or a distal volcanic source (Song and Lo, 2002; Allen et al., 2007).

### Sequence LSU 5B: 584.19–688.92 mbsf

Sequence LSU 5B, the upper sequence, represents a fundamental change in the sedimentary system both in terms of the nature and source of sediments, as well as the main depositional processes. The base of sequence LSU 5B is not marked by a sharp unconformity, hiatus, or erosive surface and was placed at 688.92 mbsf because at this depth coarse tuff beds begin to dominate. Lapilli tuff and tuff that compose most of the second sequence resemble tuff couplets described in the upper part of sequence A, although the latter are characterized by thicker beds and coarser clast size. We attribute the bulk of the LSU 5B succession to submarine explosive activity. Coarser grain size, bed thicknesses, and increase in frequency of lapilli tuff suggest an increase of explosive energy or a shift to an eruptive vent closer to the drill site.

A key volcanic feature in the core is the 2.81-m-thick lava flow (646.49–649.30 mbsf). The quenched rims on the flow, the presence of soft-sediment deformation at its base, and the analysis of bounding facies suggest that the lava flow was emplaced in a subaqueous environment. According to Walker's (1973) model, a subaerial tephritic (basaltic) lava flow with thickness similar to that cored should be fed by a vent located within 4 km from the drill site. Considering that the emplacement in water implies a higher cooling rate and several other processes that promote higher viscosity and shorter lengths, the distance of 4 km for the vent position should be considered as maximum

Despite its own relevance and significance as a time stratigraphic horizon, the occurrence of lava offers a context for interpretation of the volcanic diamictites that are in contact with this coherent flow and found at various stratigraphic levels in LSU 5B. As described here,

the volcanic diamictite is composed of juvenile lava clasts that are texturally identical to the lava flow and by pumiceous fragments similar to those composing the tuff. We interpret these diamictites as a mixture of clasts derived from autoclastic processes acting on the lava flow and clasts derived by the subaqueous explosive activity associated with the emplacement of a submarine lava flow. High-density mass flows (debris flows) related to cycles of growth and collapse of a local volcanic pile may develop in front of the lava flow so that volcanic diamictites may be found both at the base as well as above it. The presence of diamictites without related lava flows is attributed to the higher mobility of mass flows compared to lava flows. Thus diamictites are proxies for lava flows that did not reach the drill site.

A continuum exists between processes that led to the formation of eruption-fed density current deposits and lava flows; thus, these processes and resultant processes may represent different phases of the same eruption depending upon the rate of extrusion and volatile content of the magma. Eruptive activity was intermittent and likely initiated by high eruption rates and high volatile contents that favor submarine fire fountaining or subaqueous pyroclastic jets, which were transformed into eruption-fed density currents. During the late stages of these explosive eruptions lower eruption rates and diminished volatile content may produce lava flows and their associated diamictites (Stix and Gorton, 1989).

The abundant reddish oxidized fragments in lava-related diamictites and in tuffs suggest thermal oxidation conditions of high-temperature volcanic materials (Cas and Wright, 1987; Song and Lo, 2002). Oxidizing conditions can be reached either during the emergence of the volcanic vent above sea level or if the eruptive plume (or fountain) reaches and breaks the sea surface; in this sense reddish oxidized volcanic fragments may indicate the passage from a submarine eruptive environment to a shallow to emerging volcanic vent or eruption column. Further evidence of the emergence of the volcanic vent is the occurrence of stacked beds of extremely fine tuff, likely produced by contact of a vesiculating, ash-producing melt with external water, in the uppermost part of the LSU 5B (584.19–584.84 mbsf).

The presence of volcanic edifices close to the drill site was hypothesized by Wilson et al. (2007a) on the basis of the presence of large accumulation of magnetically susceptible detritus surrounding small (1–2 km wavelength), discrete, circular anomalies south of Hut Point Peninsula (Fig. 5).

The presence within the volcanic sequence of intervals composed of bioturbated, olive-green to yellowish volcanic-rich epiclastic claystone interstratified with volcanic-rich epiclastic sandstone (facies 11a; e.g., 608–618 mbsf) indicates that volcanic activity was periodically interrupted by periods of quiescence. During these periods the supply of volcaniclastic detritus was

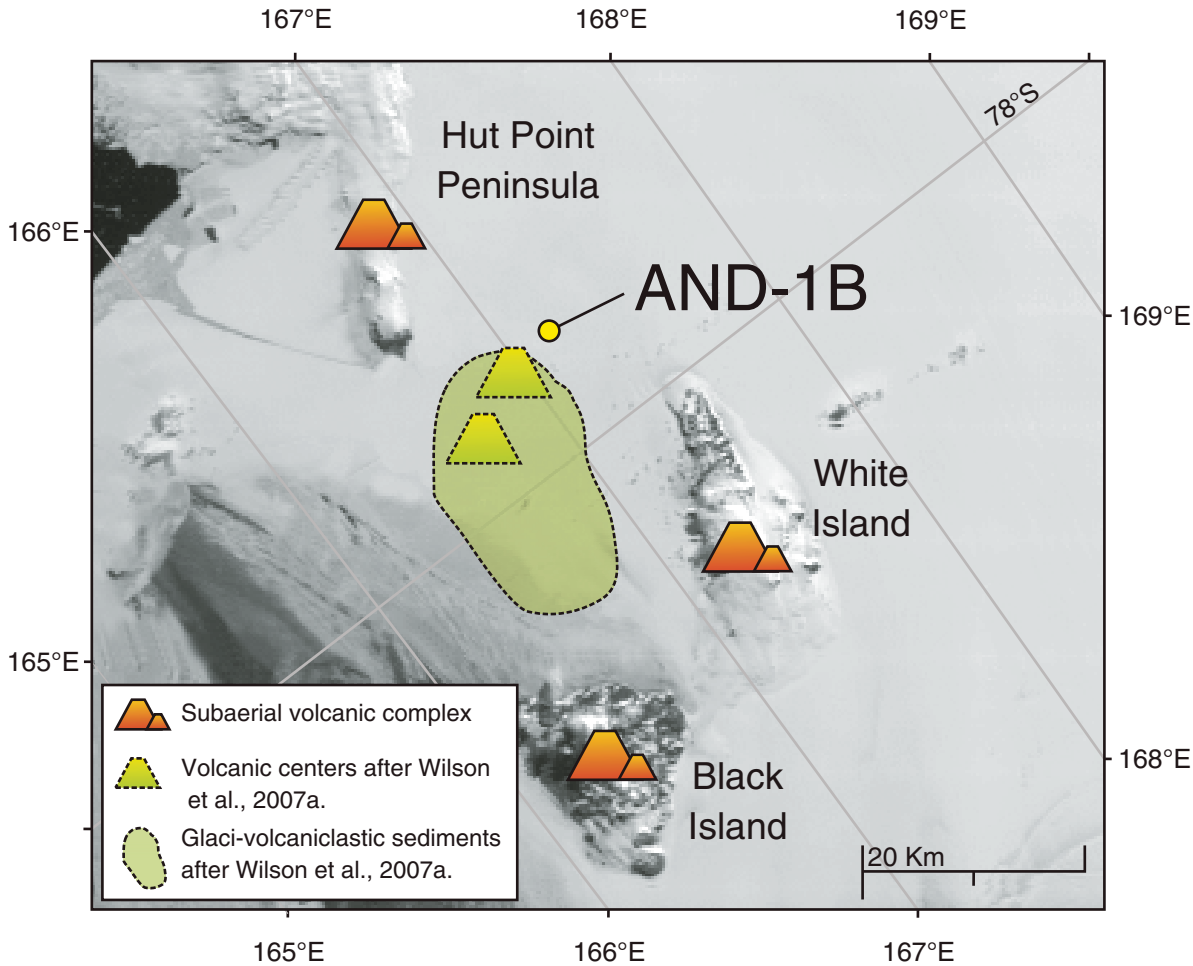


**Figure 5. Close-up from Figure 1, illustrating the position of volcanic centers and glacial-volcaniclastic sediments relative to AND-1B core site.**

reduced, whereas benthic biologic activity (bioturbation) and the deposition of epiclastic and hemipelagic sediments was favored. A representation of the depositional system is schematized in Figure 6.

## DISCUSSION

### Temporal Evolution of the Volcanic Complex in LSU 5

A well-constrained chronology has been developed for the AND-1B core from a combination of $^{40}Ar/^{39}Ar$ ages, microfossil biostratigraphy, and correlation of magnetic polarity stratigraphy with the geomagnetic polarity time scale on primary volcanic deposits for the upper ~600 m of the AND-1B core (Wilson et al., 2007c; Naish et al., 2008). The age model considers the presence of several hiatuses, changes in accumulation rate between hiatuses, and the presence of several erosion surfaces. Despite the paucity of volcanic material suitable for radiometric dating, the recognition of four well-defined time stratigraphic windows into the history and dynamics of the Ross Ice Shelf (Naish et al., 2008, 2009) has resulted. Ages of ca. 4.6–4.9 Ma and ca. 3.2–3.6 Ma were indicated for 460–600 mbsf and 280–440 mbsf, respectively, whereas ages of ca. 2.35–2.75 Ma and ca. 0.1–0.78 Ma were attributed to 150–253 mbsf and 20–80- mbsf (Naish et al., 2008, 2009). The chronology of LSU 5 is less robust below 586 mbsf due to the absence of biostratigraphic data and the fact that correlation with the geomagnetic polarity time scale is poorly constrained.

The Miocene-Pliocene boundary should occur within a series of hiatuses in LSU 5 between 615.50 and 635.00 mbsf (~620 mbsf) that account for ~1 m.y. of time (Wilson et al., 2007c). A $^{40}Ar/^{39}Ar$ age (6.48 ± 0.13 Ma) on the basaltic lava flow sampled at 648 mbsf indicates a Late Miocene age for this interval of the core. The only chronostratigraphic data available below 700 mbsf are some $^{40}Ar/^{39}Ar$ ages of volcanic clasts affording maximum depositional ages of 9.41 Ma at 796.53 mbsf, 8.53 Ma at

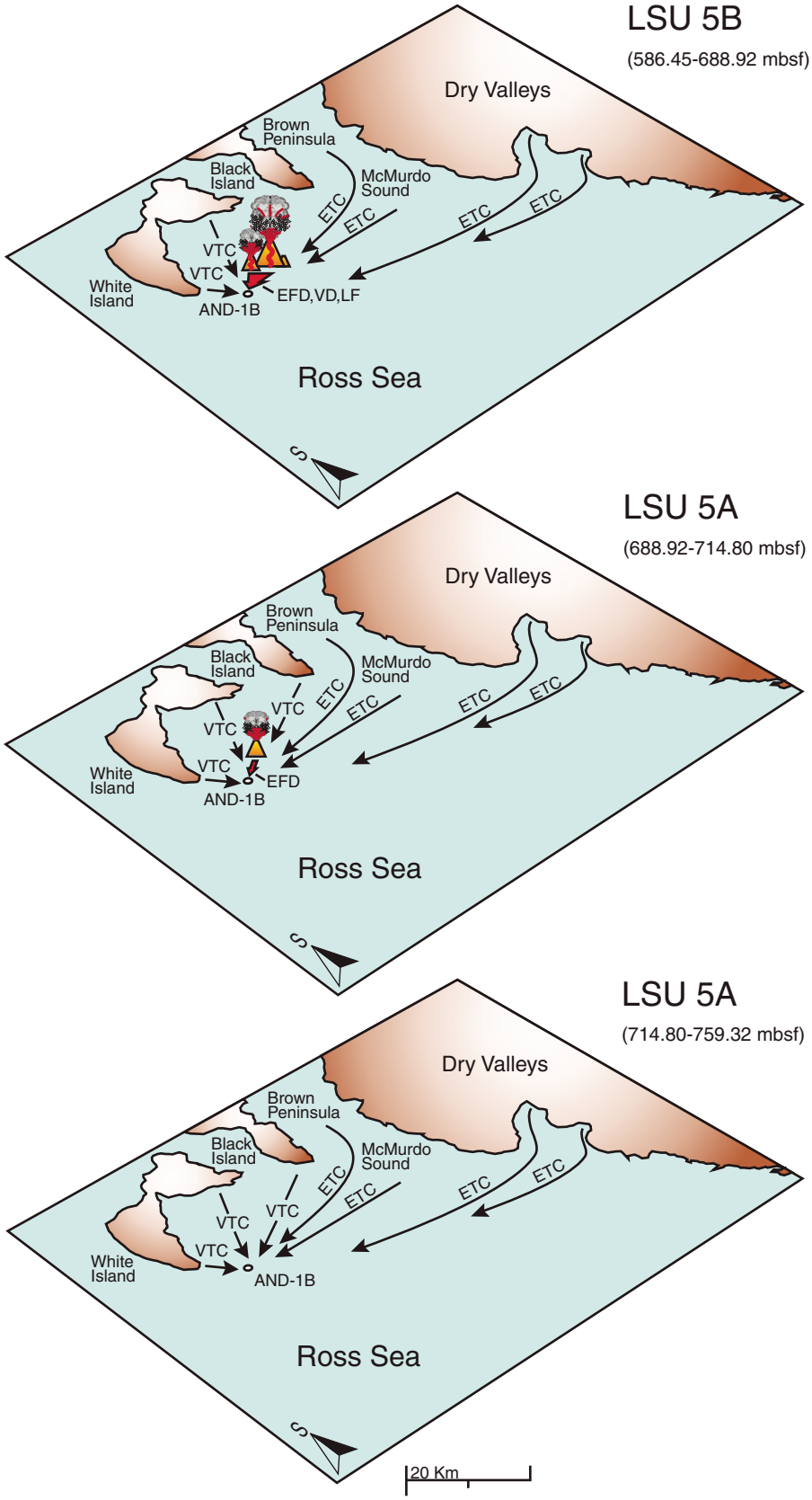


**Figure 6. Schematic models illustrating the progressive migration or growth of a volcanic edifice close to the coring site. Main eruptive, transport, and depositional processes are also sketched (see text for details); flow patterns are purely illustrative. VTC—volcanic-rich turbidity current; EFD—eruption-fed density currents; VD—volcanic diamictites; LF—lava flows; ETC—epiclastic turbidity currents; mbsf—meters below seafloor.**

822.78 mbsf, and 13.57 Ma for the base of the AND-1B drill core (Ross et al., 2007; J. Ross, 2009, personal commun.). Thus lacking any other biostratigraphic constraints, LSU 5 volcanism initiated after 8.53 Ma and ceased by 4.9 Ma. Additional, more detailed, clast dating may refine the chronology of the lower half of the core, constraining the very beginning of the volcanic activity recorded in LSU 5.

Considering the drill-site position, the LSU 5 sequence may be an expression of the currently eroded and submarine northwesternmost extension of the 7.65 ± 0.69 Ma White Island volcanic complex (Cooper et al., 2007; Wilson et al., 2007a). The general lack of siliciclastic glacial deposits and biogenic sediments interleaved with volcanic detritus is consistent with LSU 5 representing a short-lived interval. However, the occurrence of more than one paleomagnetic reversal within this LSU places some minimum constraints (i.e., hundreds of thousands of years) on the duration of volcanism (Wilson et al., 2007c).

## Structural Evolution of the Volcanic Complex in LSU 5

The onset of the LSU 5 volcanic sequence represents a significant shift from a glacier-dominated to a volcano-dominated geological system. Lithostratigraphic unit 6 (LSU 6), which underlies LSU 5 and extends to ~1225 mbsf, contains no pure volcanic horizons (Krissek et al., 2007). The activation of a new source of volcaniclastic material is indicated by the constant supply of very fine primary pyroclasts that were remobilized, reworked, and form the volcanic fraction of the distal epiclastic turbidites recovered from the lowermost part of sequence LSU 5A. The first evidence of a nearby growing volcanic complex in the McMurdo Sound basin and in LSU 5 is the eruption-fed aqueous density current deposits that are interlayered with laminated volcanic claystone and siltstone in the uppermost part of sequence LSU 5A.

Sequence LSU 5B may have resulted from an increase of eruptive energy due to higher magma supply or gas content, and/or a shift of the eruptive activity closer to the drill site. Eruptions may have been produced by very complex edifices made up of several monogenetic and closely spaced and often overlapping cones; similar structures were produced during recent basaltic eruption at many locations, including Surtsey and its associated satellites (Thorarinsson, 1964; Lorenz, 1974; Jakobsson and Moore, 1982; Kokelaar and Durant, 1983), Falcon Island, Tonga (Hoffmeister et al., 1929), and Capelinhos or São Roque volcano, Azores (Machado et al., 1962; Cole et al., 1996, 2001; Solgevik et al., 2007; Zanon et al., 2008). Similar volcanic complexes have also been inferred from ancient volcanic sequences like Lookout Bluff, New Zealand (Maicher, 2003), Pahvant Butte, Utah (White, 1996, 2001), and Kangerluluk sequence, southeast Greenland (Mueller et al., 2000, 2002).

Our interpretations of facies associations in LSU 5 suggest that a single eruption (or eruptive period) started with a high-energy phase with the deposition of lapilli tuff and tuff, followed by effusive emission of lava flows and related volcanic diamictites when the energy or gas content decreased. Single eruptive events were likely short-lived, with activity commonly lasting from days to a few years. Observations at Surtsey and Capelinhos indicate that eruptions lasting several days to a few weeks constructed edifices as big as 180 m above the sea level (>300 m above seafloor) (Thorarinsson et al., 1964; Machado et al., 1962). Analogous to these observed eruptions, the LSU 5 activity could have been cyclical, intermittent, and alternating with quiescent periods during which erosion of primary volcanic deposits and deposition of epiclastic turbidites occurred. The growth of the volcanic complex may have continued until the emergence of the volcanic complex or until the establishment of a very shallow water setting, as testified by high-temperature oxidization products that are abundant in the sequence.

In the topmost part of sequence LSU 5B, a series of hiatuses occur mainly within volcanic-rich epiclastic deposits (wavy dashed red line in Fig. 2), indicating that volcanic activity was repeatedly interrupted by variably long periods of quiescence. During quiescence, erosion of volcanic deposits and epiclastic deposition occurred. The duration of these periods of reduced volcanic activity cannot be exactly constrained since biostratigraphic data are absent in this part of the core and correlation with the geomagnetic polarity time scale is poorly constrained. However, an overall duration of ~1 m.y. of time was reconstructed on the basis of stratigraphic considerations and geochronologic data (Wilson et al., 2007c).

## Paleoclimatic and Paleoenvironmental Implications

Facies analysis and interpretation of LSU 5 provide important data for paleoclimate and paleoenvironment reconstructions. Sequence LSU 5A is bounded at its base by deposits that indicate subglacial conditions with oscillation of the grounding line and variable influence of icebergs in sediment delivery (LSU 6 and LSU 7). According to Krissek et al. (2007), these oscillations were accompanied by high sedimentation rates with submarine outwash and mass-flow deposition. The contact between LSU 6 and LSU 5 represents the onset of a long period of ice retreat from the AND-1B core site. The retreat is coincident with a rapid reduction to zero in outsized clast (dropstone) abundance of both volcanic and Transantarctic Mountain basement origin that is observed in LSU 5A (Talarico and Sandroni, 2009). The volcanic record of LSU 5 is unusual in the context of the AND-1B succession in that evidence for interruptions by glaciations is absent.

We infer open-water conditions at the time of the volcanic eruptions documented in LSU 5B. The emergence of a submarine volcano or generation of subaqueous pyroclastic jets that break the water surface preclude significant ice cover. During terrestrial subglacial eruptions the heat is more or less efficiently transferred from the erupted magma to the surrounding glacier (55% to >80%; Höskuldsson and Sparks, 1997; Gudmundsson, 2003; Gudmundsson and Cook, 2004; Gudmundsson et al., 2004) while warm water derived from ice melting remains confined in a water-filled cavity in the glacier until it can escape through fractures or permeable ice layers. If an eruption persists, the subglacial volcano can break the ice surface and emerge, melting as much as several hundreds of meters of ice (Höskuldsson and Sparks, 1997). By contrast, in submarine eruptions the heat transfer to the overlying ice is likely much less efficient since a significant part of magma heat is lost during the interaction with seawater and the water eventually produced by ice melting quickly cools and moves away. The presence of a thick ice shelf would likely prevent the emergence of the volcano and favor exclusively subaqueous activity. Thus a deglaciated condition above the drill site seems more realistic for the primary volcanic sequences of LSU 5B. The lack of dropstones and glacial diamictite in LSU 5 supports this interpretation.

These considerations seem to be in agreement with data on marine oxygen isotope ($\delta^{18}O$) records from diatomite deposits overlying LSU 5 that indicate higher global sea surface temperatures relative to today, with open-water conditions or thin ice cover in the Ross Embayment following the deposition of the volcanic sequence (Naish et al., 2009). The volcanic activity may have continued until the emergence of the volcanic complex, as testified by abundant oxidized volcanic fragments both in tuff and in volcanic diamictite deposits.

The hypothesis of an emerging volcano seems at first appearance to be unrealistic in light of the current basin bathymetry and considering an eruptive style as that inferred by the sequence interpretation (Surtseyan style).

Today, a volcano erupting on the seafloor close to the AND-1B would need to grow vertically ~1000 m to be in shallow water or an emergent environment. However, the present basin configuration is the result of the loading of the crust by the Ross Island volcanic pile that produced ~1 km of subsidence beneath Ross Island and the development of an enclosing moat (Stern et al., 1991) superimposed on the regional pattern of accommodation space created by late Cenozoic rifting (Naish et al. 2007). At the time that LSU 5 deposition began, the Ross Island volcanic complex was most likely not present, as the oldest outcrops at Mount Bird are 4.6 Ma (Wright and Kyle, 1990a), and Mount Erebus, composing the bulk of the island, is younger than 1.3 Ma. If Ross Island were absent during the LSU 5 deposition, then only regional subsidence related to the late Cenozoic rifting was responsible for the basin configuration. Removing the ~1 km of subsidence due to Ross Island loading results in a shallow water or emerged setting for the volcanic complex that produced LSU 5B, which is consistent with the presence of oxidized volcanic fragments in the core.

## CONCLUSIONS

Our new detailed volcano-stratigraphic data and interpretations of the thick and very complex volcaniclastic sequence in the AND-1B core provide new insights into the volcanic history and evolution of the Erebus Volcanic Province during the Late Miocene. This study presents a record and a model of submarine volcanism in the intracontinental rift setting of the Ross Embayment. The study of the LSU 5 volcanic sequence enabled us to identify mechanisms of transport and deposition of volcaniclastic detritus during a time of minimal ice cover followed by the development of a new volcanic complex prior to 6.48 Ma. This volcanic complex began erupting in submarine conditions and continued until the volcanic complex summit grew into a very shallow water environment. According to our interpretation, eruptive dynamics were similar to those characterizing recent shallow-water basaltic eruptions that have been observed in several geologic settings. The sequence was probably deposited during repeated short-lived eruptive events; each event likely started with a high-energy phase during which the deposition of lapilli tuff and tuff occurred, followed by effusive emission of lava flows and related volcanic diamictites and other gravity flow deposits. More generally, the analysis of the LSU 5 volcanic sequence in the AND-1B core furnishes a new and consistent data set for the study of basaltic submarine volcanic activity and its products. The facies analysis and interpretation of the LSU 5 volcaniclastic sequence preclude any interaction with grounded or ungrounded ice, indicating prevalent open water conditions (or at maximum seasonal sea ice).

### ACKNOWLEDGMENTS

The ANDRILL project is a multinational collaboration between the Antarctic programs of Germany, Italy, New Zealand, and the United States. Antarctica New Zealand is the project operator and developed the drilling system in collaboration with A. Pyne. Antarctica New Zealand supported the drilling team at Scott Base; Raytheon Polar Services Corporation supported the science team at McMurdo Station and the Crary Science and Engineering Laboratory. The ANDRILL Science Management Office at the University of Nebraska-Lincoln provided science planning and operational support. The scientific studies are jointly supported by the U.S. National Science Foundation, the New Zealand Foundation for Research Science and Technology, the Italian Antarctic Research Programme, the German Research Foundation, and the Alfred Wegener Institute for Polar and Marine Research. We are grateful for the detailed core logging by the McMurdo Ice Shelf Sedimentology Team and for helpful discussions with Phil Kyle during the drilling. We thank co-chiefs (Tim Naish, Ross Powell) and staff scientist Richard Levy for coordinating efforts, and A. Cavallo (Istituto Nazionale di Geofisica e Vulcanologia, Rome) for assistance in scanning electron microscope observations. Di Roberto benefited from a Programme for Antarctic Research post-doctoral fellowship.

### REFERENCES CITED

Allen, S.R., Hayward, B.W., and Mathews, E., 2007, A facies model for a submarine volcaniclastic apron: The Miocene Manukau Subgroup, New Zealand: Geological Society of America Bulletin, v. 119, p. 725–742, doi: 10.1130/B26066.1.

Armienti, P., Tamponi, M., and Pompilio, M., 2001, Sand provenance from major and trace element analyses of bulk rock and sand grains from CRP-2/2A, Victoria Land Basin, Antarctica: Terra Antarctica, v. 8, p. 569–582.

Armstrong, R.L., 1978, K-Ar dating: Late Cenozoic McMurdo Volcanic Group and Dry Valley glacial history, Victoria Land, Antarctica: New Zealand Journal of Geology and Geophysics, v. 21, p. 685–698.

Associated Press, 2009, Tongan inspectors head to undersea volcano: http://www.physorg.com/news156663985.html.

Cas, R.A.F., and Wright, J.V., 1987, Volcanic successions: London, Allen and Unwin, 528 p.

Cashman, K.V., and Fiske, R.S., 1991, Fallout of pyroclastic debris from submarine volcanic eruptions: Science, v. 253, p. 275–280, doi: 10.1126/science.253.5017.275.

Cole, P.D., Guest, J.E., and Duncan, A.M., 1996, Capelinhos: The disappearing volcano: Geology Today, v. 12, p. 68–72, doi: 10.1046/j.1365-2451.1996.00010.x.

Cole, P.D., Guest, J.E., Duncan, A., and Pacheco, J.M., 2001, Capelinhos 1957–1958, Faial, Azores: Deposits formed by an emergent Surtseyan eruption: Bulletin of Volcanology, v. 63, p. 204–220, doi: 10.1007/s004450100136.

Cooper, A.F., Adam, L.J., Coulter, R.F., Eby, G.N., and McIntosh, W.C., 2007, Geology, geochronology and geochemistry of a basanitic volcano, White Island, Ross Sea, Antarctica: Journal of Volcanology and Geothermal Research, v. 165, p. 189–216, doi: 10.1016/j.jvolgeores.2007.06.003.

Doucet, P., Mueller, W., and Chartrand, F., 1994, Archean, deepwater, volcanic eruptive products associated with the Coniagas massive deposit, Quebec, Canada: Canadian Journal of Earth Sciences, v. 31, p. 1569–1584.

Esser, R.P., Kyle, P.R., and McIntosh, W.C., 2004, 40Ar/39Ar dating of the eruptive history of Mt. Erebus, Antarctica: Volcano evolution: Bulletin of Volcanology, v. 66, p. 671–686, doi: 10.1007/s00445-004-0354-x.

Fargo, A.J., McIntosh, W.C., Dunbar, N.W., and Wilch, T.I., 2008, 40Ar/39Ar geochronology of Minna Bluff, Antarctica: Timing of Mid-Miocene glacial erosional events within the Ross Embayment: Eos (Transactions, American Geophysical Union), v. 89, Fall meeting supplement, abs. V13C-2127.

Fiske, R.S., 1963, Subaqueous pyroclastic flows in the Ohanapecosh Formation, Washington: Geological Society of America Bulletin, v. 74, p. 391–406, doi: 10.1130/0016-7606(1963)74[391:SPFITO]2.0.CO;2.

Fiske, R.S., Cashman, K.V., Shibata, A., and Watanabe, K., 1998, Tephra dispersal from Myojinsho, Japan, during its shallow submarine eruption of 1952–1953: Bulletin of Volcanology, v. 59, p. 262–275, doi: 10.1007/s004450050190.

Gudmundsson, M.T., 2003, Melting of ice by magma-ice-water interactions during subglacial eruptions as an indicator of heat transfer in subaqueous eruptions, *in* White, J.D.L, et al., eds., Explosive subaqueous volcanism: American Geophysical Union Geophysical Monograph 140, p. 61–72.

Gudmundsson, M.T., and Cook, K., 2004, The 1918 eruption of Katla, Iceland: Magma flow rates, ice melting rates and generation of the greatest jökulhlaup of the 20th century: General Assembly 2004, International Association of Volcanology and Chemistry of the Earth's Interior, Puco´n, Chile, 14–19 November, Abstract s11b_pth_135.

Gudmundsson, M.T., Sigmundsson, F., Björnsson, H., and Högnadóttir, T., 2004, The 1996 eruption at Gjálp, Vatnajökull ice cap, Iceland: Efficiency of heat transfer, ice deformation and subglacial water pressure: Bulletin of Volcanology, v. 66, p. 46–65, doi: 10.1007/s00445-003-0295-9.

Hoffmeister, J.E., Ladd, H.S., and Ailing, H.L., 1929, Falcon Island: American Journal of Science, v. 18, p. 461–471.

Höskuldsson, A., and Sparks, R.S.J., 1997, Thermodynamics and fluid dynamics of effusive sub-glacial eruptions: Bulletin of Volcanology, v. 59, p. 219–230, doi: 10.1007/s004450050187.

Jakobsson, S.P., and Moore, J.G., 1982, The Surtsey Research Drilling Project of 1979: Surtsey Research Progress Report, v. 9, p. 76–93.

Kokelaar, B.P., 1983, The mechanism of Surtseyan volcanism: Geological Society of London Journal, v. 140, p. 939–944, doi: 10.1144/gsjgs.140.6.0939.

Kokelaar, B.P., and Busby, C., 1992, Subaqueous explosive eruption and welding of pyroclastic deposits: Science, v. 257, p. 196–201, doi: 10.1126/science.257.5067.196.

Kokelaar, B.P., and Durant, G.P., 1983, The submarine eruption and erosion of Surtla (Surtsey), Iceland: Journal of Volcanology and Geothermal Research, v. 19, p. 239–246, doi: 10.1016/0377-0273(83)90112-9.

Krissek, L., Browne, G., Carter, L., Cowan, E., Dunbar, G., McKay, R., Naish, T., Powell, R., Reed, J., Wilch, T., and The ANDRILL-MIS Science Team, 2007, Sedimentology and stratigraphy of the AND-1B Core, ANDRILL McMurdo Ice Shelf Project, Antarctica: Terra Antartica, v. 14, no. 3, p. 185–222.

Kyle, P.R., 1977, Mineralogy and glass chemistry of recent volcanic ejecta from Mt. Erebus, Ross Island, Antarctica: New Zealand Journal of Geology and Geophysics, v. 20, p. 1123–1146.

Kyle, P.R., 1981, Glacial history of the McMurdo Sound area, as indicated by the distribution and nature of McMurdo volcanic rocks in the Dry Valley Drilling Project, *in* McGinnis, L.D., ed., Dry Valley Drilling Project: American Geophysical Union Antarctic Research Series, v. 33, p. 403–412.

Kyle, P.R., 1990, McMurdo volcanic group—Western Ross Embayment, *in* LeMasurier, W.E., and Thomson, J.W., eds., Volcanoes of the Antarctic plate and southern oceans: American Geophysical Union Antarctic Research Series, v. 48, p. 19–25.

Kyle, P.R., and Muncy, H.L., 1989, Geology and geochronology of McMurdo Volcanic Group rocks in the vicinity of Lake Morning, McMurdo Sound, Antarctica: Antarctic Science, v. 1, p. 345–350, doi: 10.1017/S0954102089000520.

Kyle, P.R., Moore, J.A., and Thirwall, M.F., 1992, Petrologic evolution of anorthoclase phonolite lavas at Mt. Erebus, Ross Island, Antarctica: Journal of Petrology, v. 33, p. 849–875.

Lorenz, V., 1974, Studies of the Surtsey tephra deposits: Surtsey Research Progress Report, v. 7, p. 72–79.

Machado, F., Parsons, W.H., Richards, A.F., and Mulford, J.W., 1962, Capelinhos eruption of Fayal volcano, Azores, 1957–1958: Journal of Geophysical Research, v. 67, p. 3519–3529, doi: 10.1029/JZ067i009p03519.

Maicher, D., 2003, A cluster of Surtseyan volcanoes at Lookout Bluff, North Otago, New Zealand: Aspects of edifice spacing and time, *in* White, J.D.L, et al., eds., Explosive subaqueous volcanism: American Geophysical Union Geophysical Monograph 140, p. 167–178.

Martin, U., and White, J.D.L., 2001, Depositional and eruptive mechanisms of density current deposits from a submarine vent at the Otago Peninsula, New Zealand, *in* McCaffrey, W.D., et al., eds., Particulate gravity currents: International Association of Sedimentologists Special Publication 31, p. 245–261.

Martin, U., Cooper, A.F., and Dunlap, W.J., 2009, Geochronology of Mount Morning, Antarctica: Two-phase evolution of a long-lived trachyte-basanite-phonolite eruptive center: Bulletin of Volcanology, v. 72, p. 357–371, doi: 10.1007/s00445-009-0319-1.

McIntosh, W.C., 2001, 40Ar/39Ar geochronology of tephra and volcanic clasts in CRP-2A, Victoria Land Basin, Antarctica, *in* Barrett, P.J., and Ricci, C.A., eds., Studies from the Cape Roberts Project, Ross Sea, Antarctica, Scientific report of CRP-2/2A: Terra Antartica, v. 7, p. 621–630.

McKay, R., Browne, G., Carter, L., Cowan, E., Dunbar, G., Krissek, L., Naish, T., Powell, R., Reed, J., Talarico, F., and Wilch, T., 2009, The stratigraphic signature of late Cenozoic oscillations of the Antarctic Ice Sheet in the Ross Embayment, Antarctica: Geological Society of America Bulletin, v. 121, p. 1537–1561, doi: 10.1130/B26540.1.

Mueller, W.U., 2003, A subaqueous eruption model for shallow-water, small volume eruptions: Evidence from two Precambrian examples, *in* White, J.D.L, et al., eds., Explosive subaqueous volcanism: American Geophysical Union Geophysical Monograph 140, p. 189–203.

Mueller, W.U., and White, J.D.L., 1992, Felsic fire-fountaining beneath Archean seas: Pyroclastic deposits of the 2730 MA Hunter Mine Group, Quebec, Canada: Journal of Volcanology and Geothermal Research, v. 54, p. 117–134, doi: 10.1016/0377-0273(92)90118-W.

Mueller, W.U., Garde, A.A., and Stendal, H., 2000, Shallow-water, eruption-fed, mafic pyroclastic deposits along a Paleoproterozoic coastline: Kangerluluk volcano-sedimentary sequence, southeast Greenland: Precambrian Research, v. 101, p. 163–192, doi: 10.1016/S0301-9268(99)00087-X.

Mueller, W.U., Dostal, J., and Stendal, H., 2002, Inferred Palaeoproterozoic arc rifting along a consuming plate margin: Insights from the stratigraphy, volcanology and geochemistry of the Kangerluluk sequence, southeast Greenland: International Journal of Earth Sciences, v. 91, p. 209–230, doi: 10.1007/s005310100211.

Naish, T.R., and 16 others, 2006, ANDRILL McMurdo Ice Shelf Project Scientific Prospectus: Science Management Office, University of Nebraska-Lincoln, ANDRILL Contribution 4, p. 1–18.

Naish, T.R., Powell, R.D., Levy, R., Henrys, S., Krissek, L., Niessen, F., Pompilio, M., Scherer, R., Wilson, G., and The ANDRILL-MIS Science Team, 2007, Synthesis of the Initial Scientific Results of the MIS Project (AND-1B Core), Victoria Land Basin, Antarctica: Terra Antartica, v. 14, p. 317–327.

Naish, T.R., Powell, R.D., Barrett, P.J., Levy, R.H., Henry, S., Wilson, G.S., Krissek, L.A., Niessen, F., Pompilio, M., Ross, J., Scherer, R., Talarico, F., Pyne, A., and the ANDRILL-MIS Science Team, 2008, Late Neogene climate history of the Ross Embayment from the AND-1B drill core: Culmination of three decades of Antarctic margin drilling, *in* Cooper, A.K., ed., Antarctica: A keystone in a changing world, Proceedings of the 10th International Symposium on Antarctic Earth Sciences: Washington, D.C., National Academies Press, p. 71–82.

Naish, T., and 55 others, 2009, Obliquity-paced Pliocene West Antarctic Ice Sheet oscillations: Nature, v. 458, p. 322–328, doi: 10.1038/nature07867.

Pompilio, M., Dunbar, N., Gebhardt, A.C., Helling, D., Kuhn, G., Kyle, P., McKay, R., Talarico, F., Tulaczyk, S., Vogel, S., Wilch T., and The ANDRILL-MIS Science Team, 2007, Petrology and geochemistry of the AND-1B Core, ANDRILL McMurdo Ice Shelf Project, Antarctica: Terra Antartica, v. 14, p. 255–288.

Rao, A., Chen, Y., Lee, S., Leigh, J., Johnson, A., and Renambot, L., 2006, Corelyzer: Scalable geologic core visualization using OSX, Java and OpenGL: Apple's Worldwide Developers Conference 2006: Electronic Visualization Laboratory, http://www.evl.uic.edu/core.php?mod=4&type=3&indi=310.

Ross, J., McIntosh, W.C., Dunbar, N.W., and ANDRILL-MIS Science Team Preliminary, 2007, 40Ar/39Ar results from the AND-1B core, *in* Cooper, A.K., et al., eds., Antarctica: A keystone in a changing world: Online Proceedings of the 10th ISAES X: U.S. Geological Survey Open-File Report 1047, extended abs. 093.

Skilling, I.P., 1994, Evolution of an englacial volcano—Brown Bluff, Antarctica: Bulletin of Volcanology, v. 56, p. 573–591, doi: 10.1007/BF00302837.

Smellie, J.L., 1999, Subglacial eruptions, *in* Sigurdsson, H., et al., eds., Encyclopedia of volcanoes: San Diego, Academic Press, p. 403–418.

Smellie, J.L., and Hole, M.J., 1997, Products and processes in Pliocene-recent, subaqueous to emergent volcanism in the Antarctic Peninsula: Examples of englacial Surtseyan volcano construction: Bulletin of Volcanology, v. 58, p. 628–646, doi: 10.1007/s004450050167.

Solgevik, H., Mattsson, H.B., and Hermelin, O., 2007, Growth of an emergent tuff cone: Fragmentation and depositional processes recorded in the Capelas tuff cone, São Miguel, Azores: Journal of Volcanology and Geothermal Research, v. 159, p. 246–266, doi: 10.1016/j.jvolgeores.2006.06.020.

Song, S.R., and Lo, H.J., 2002, Lithofacies of volcanic rocks in the central Coastal Range, eastern Taiwan: Implications for island arc evolution: Journal of Asian Earth Sciences, v. 21, p. 23–38, doi: 10.1016/S1367-9120(02)00003-2.

Stern, T.A., Davey, F.J., and Delisle, G., 1991, Lithospheric flexure induced by the load of the Ross Archipelago, southern Victoria Land, Antarctica, *in* Thomson, M.R.A., et al., eds., Geological evolution of Antarctica: Cambridge, Cambridge University Press, p. 323–328.

Stix, J., and Gorton, M.P., 1989, Subaqueous volcaniclastic rocks of the Confederation lake area, northwestern Ontario: Discrimination between pyroclastic and epiclastic emplacement: Ontario Geological Survey Miscellaneous Paper, v. 143, p. 83–93.

Talarico, F., and Sandroni, S., 2009, Provenance signatures of the Antarctic Ice Sheets in the Ross Embayment during the Late Miocene to Early Pliocene: The ANDRILL AND-1B core record: Global and Planetary Change, v. 69, p. 103–123, doi: 10.1016/j.gloplacha.2009.04.007.

Thorarinsson, S., 1964, Surtsey. The new island in the North Atlantic: New York, Viking Press, 63 p.

Walker, P.L., 1973, Lengths of lava flows: Royal Society of London Philosophical Transactions, v. 274, p. 107–118.

White, J.D.L., 1996, Pre-emergent construction of a lacustrine basaltic volcano, Pahvant Butte: Bulletin of Volcanology, v. 58, p. 249–262, doi: 10.1007/s004450050138.

White, J.D.L., 2000, Subaqueous eruption-fed density currents and their deposits: Precambrian Research, v. 101, p. 87–109, doi: 10.1016/S0301-9268(99)00096-0.

White, J.D.L., 2001, Eruption and reshaping of Pahvant Butte volcano in Pleistocene Lake Bonneville, *in* White, J.D.L., and Riggs, N.R., eds., Volcaniclastic sedimentation in lacustrine settings: International Association of Sedimentologists Special Publication 30, p. 61–80.

White, J.D.L., and Houghton, B.F., 1999, Surtseyan and related eruptions, *in* Sigurdsson, H., et al., eds., Encyclopedia of volcanoes: San Diego, Academic Press, p. 495–512.

White, J.D.L., and Houghton, B.F., 2006, Primary volcaniclastic rocks: Geology, v. 34, p. 677–680, doi: 10.1130/G22346.1.

Wilch, T.I., McIntosh, W.C., Panter, K.S., Dunbar, N.W., Smellie, J.L., Fargo, A., Scanlan, M., Zimmerer, M.J., Ross, J., and Bosket, M.E., 2008, Volcanic and glacial geology of the Miocene Minna Bluff Volcanic Complex, Antarctica: Eos (Transactions, American Geophysical Union), v. 89, Fall Meeting supplement, abs.V11F–06.

Wilson, G., Damaske, D., Moeller, H.D., Tinto, K., and Jordan, T., 2007a, The geological evolution of southern McMurdo Sound—New evidence from a high-resolution aeromagnetic survey: Geophysical Journal International, v. 170, p. 93–100, doi: 10.1111/j.1365-246X.2007.03395.x.

Wilson, G., Florindo, F., Sagnotti, L., Ohneiser, C., and the ANDRILL-MIS Science Team, 2007b, Paleomagnetism of the AND-1B Core, ANDRILL McMurdo Ice Shelf Project, Antarctica: Terra Antartica, v. 14, p. 289–296.

Wilson, G., 20 others, and the ANDRILL-MIS Science Team, 2007c, Preliminary integrated chronostratigraphy of the AND-1B Core, Andrill McMurdo ice shelf project, Antarctica: Terra Antartica, v. 14, p. 297–316.

Wright, A.C., and Kyle, P.R.A., 1990a, Mount Bird, *in* LeMasurier, W.E., and Thomson, J.W., eds., Volcanoes of the Antarctic plate and southern oceans: American Geophysical Union Antarctic Research Series, v. 48, p. 97–98.

Wright, A.C., and Kyle, P.R.A., 1990b, Mount Terror, *in* LeMasurier, W.E., and Thomson, J.W., eds., Volcanoes of the Antarctic plate and southern oceans: American Geophysical Union Antarctic Research Series, v. 48, p. 99–102.

Zanon, V., Pacheco, J., and Pimentel, A., 2008, Growth and evolution of an emergent tuff cone: Considerations from structural geology, geomorphology and facies analysis of São Roque volcano, São Miguel (Azores): Journal of Volcanology and Geothermal Research, v. 180, p. 277–291, doi: 10.1016/j.jvolgeores.2008.09.018.

Manuscript Received 31 July 2009
Revised Manuscript Received 12 January 2010
Manuscript Accepted 14 January 2010